

Design and Synthesis of Two-Dimensional Pillared MOF Layers by Connecting Infinite One-Dimensional Chains via 4,4'-Bipyridine¹

L. J. Li*, L. Z. Wang, X. Y. Yang, G. Y. Wang, Ch. Tian, and J. L. Du

Key Laboratory of Chemical Biology of Hebei Province, Hebei University, Baoding, 071002 P.R. China

*e-mail: llj@hbu.edu.cn

Received September 13, 2011

Abstract—Two novel metal-organic frameworks, $[\text{Cd}(\text{Bna})(\text{DMF})_2(\text{H}_2\text{O})_2]_n \cdot n\text{DMF}$ (**I**) (Bna = 2,2'-dihydroxy-1,1'-dinaphthyl-3,3'-dicarboxylate) and $[\text{Cd}(\text{Bna})(\text{Bipy})(\text{DMF})_2]_n$ (**II**) (Bipy = 4,4'-bipyridine) have been synthesized under mild conditions and structurally characterized. Crystal structural analyses reveal that complex **I** adopts a 1D spiral structure with DMF guest molecules in the spiral by hydrogen bondings. Complex **II** is constructed by $-\text{Cd}-\text{Bna}-\text{Cd}-$ zigzag chains, which are further connected by Bipy into a 2D sheet. X-ray powder diffraction and thermogravimetric analyses for **I** and **II** show that they are highly thermally stable in the solid state.

DOI: 10.1134/S1070328413030056

INTRODUCTION

Great progress has been made during the past two decades in the construction of metal-organic frameworks (MOFs) comprising an infinite alternate arrangement of metal ions and bridging ligands [1–3]. Because of the ability to systematically tune their porosity and the functionalities that are incorporated within the framework scaffolds [4–9]. As a result, numerous MOFs have been engineered for a number of potential applications, including gas storage [10–13], nonlinear optics [8], and catalysis [14, 15]. Lin group have particularly demonstrated the utility of binaphthyl-derived homochiral MOFs in heterogeneous asymmetric catalysis [16, 17]. Although a number of strategies have been developed to achieve 2D or 3D structures MOFs in recent years [9] it is still a challenge to obtain MOFs with open channels and extremely large porosity. Modification of the frameworks are still attracting much interest.

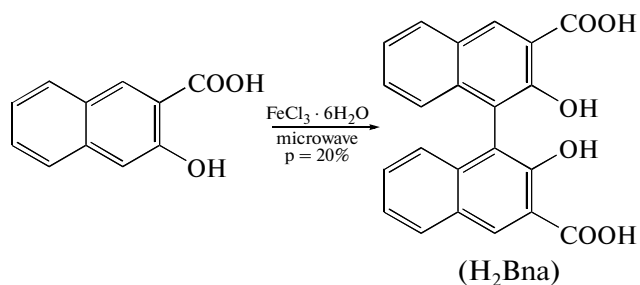
Presently, we have been interested in constructing 2D structures MOFs containing Bna ligands, where $\text{H}_2\text{Bna} = 2,2'$ -dihydroxy-1,1'-dinaphthyl-3,3'-dicarboxylic acid, contributing to asymmetric synthesis. The design strategy is to link 1D chains, made of the combination of Bna and metal ion, to each other by using a linear ligand to form MOFs layers. The chains can be combined through linear bifunctional ligand such as 4,4'-bipyridine (Bipy) to generate 2D MOFs architecture.

EXPERIMENTAL

Materials and methods. All chemicals were purchased commercially and used without further puri-

cation. Infrared spectra were obtained with a Nicolet Impact 410 FTIR spectrometer in the range 400–4000 cm^{-1} using the KBr pellets. A PerkinElmer TGA thermogravimetric analyzer was used to obtain thermogravimetric analysis (TGA) curve in air with a heating rate of 20°C/min. ¹H NMR spectra were run at 25°C using a Bruker 400 (400 MHz) spectrometer. X-ray powder diffraction (XRPD) spectra were obtained with a Bruker D8 ADVANCE.

Synthesis of H_2Bna carried out according to the following scheme:



A mixture of 3-hydroxy-2-naphthoic acid (9.4 g, 50 mmol) and $\text{FeCl}_3 \cdot 6\text{H}_2\text{O}$ (20.3 g, 56 mmol) was grinded sufficiently, the mixture was conducted in microwave tube at 70°C and 700 W for 35 min. The mixture was kept at room temperature with occasional grinding for a certain period of the reaction time until the reaction was completed. The residue was purified by column chromatography on silica gel with petroleum ether–ethyl acetate (5 : 1) to afford the product H_2Bna in 74% yield (7.0 g). Mp > 290°C; ¹H NMR ($(\text{CD}_3)_2\text{CO}$; 400 MHz; δ , ppm): 7.14–7.17 (m., 2H, Ar–H), 7.39–7.42 (m., 4H, Ar–H), 8.09–8.11 (m., 2H, Ar–H), 8.84 (s., 2H, Ar–H); IR (KBr; ν , cm^{-1}):

¹ The article is published in the original.

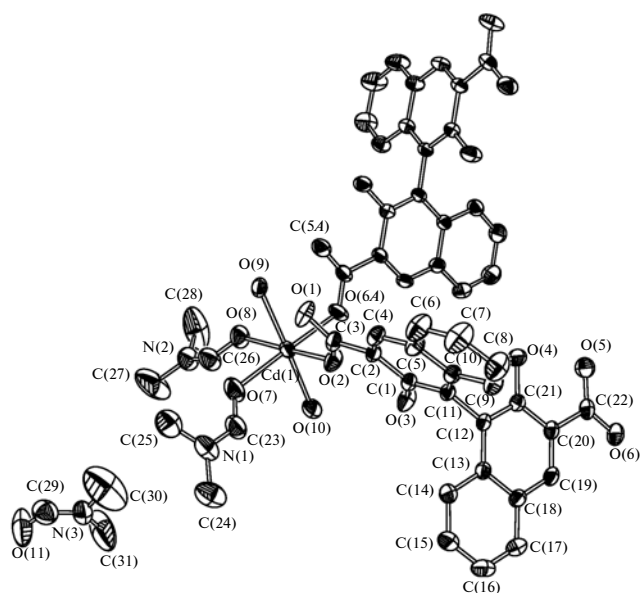


Fig. 1. The coordination environment around Cd(II) in **I** with the thermal ellipsoid at the 30% probability level. Symmetry code: (A) $-x - 1/2, y - 1/2, -z + 1/2$.

3059, 1661, 1499, 1455, 1272, 1228, 1150, 1072, 886, 796, 736.

For $C_{22}H_{14}O_6$

anal. calcd., %: C, 81.48; H, 2.36.

Found, %: C, 81.62; H, 2.28.

Synthesis of $[Cd(Bna)(DMF)_2(H_2O)_2]_n \cdot nDMF$ (**I**).

A mixture of H_2Bna (7.5 mg, 0.02 mmol) and NaOH (1.6 mg, 0.04 mmol) was warmed to dissolved in 5 mL ethanol. After removing the solvents under a reduced pressure, the residue was dissolved in 2 mL DMSO as the under layer in a tube. A mixture of 1 mL DMSO and H_2O (1 : 1) was carefully layered as the middle layer in the tube. 24.2 mg (0.08 mmol) $Cd(NO_3)_2 \cdot 6H_2O$ was dissolved in 2 mL DMF and H_2O (1 : 1) as the up layer. The tube was then sealed. Diffusion between the three phases over a period produced transparent block colourless crystals of **I**. IR (KBr; ν , cm^{-1}): 1658, 1570, 1461, 1392, 1309, 1018, 940, 861, 751, 599.

For $C_{31}H_{37}N_3O_{11}Cd$

anal. calcd., %: C, 50.24; H, 5.00; N, 5.68; Cd, 15.19.

Found, %: C, 50.33; H, 4.86; N, 5.48; Cd, 15.15.

Synthesis of $[Cd(Bna)_2(Bipy)(DMF)_2]_n$ (II**).** 34 mg (0.12 mmol) $Cd(NO_3)_2 \cdot 4H_2O$ was dissolved in a mixture of 2 mL DMSO and H_2O ($v/v = 1/2$) as the under layer in a tube. A mixture of 1 mL DMF and H_2O ($v/v = 1/1$) was carefully layered as the middle layer in the tube. A mixture of H_2Bna (7.5 mg, 0.02 mmol) and 8 mg (0.04 mmol) Bipy was dissolved in 2 mL DMF as

the up layer. The tube was then sealed. Diffusion between the three phases over a period of 3 months produced transparent rhombic block crystals of **II**. IR (KBr; ν , cm^{-1}): 1640, 1581, 1399, 1455, 1110, 1110, 816, 758, 673, 598.

For $C_{38}H_{34}N_4O_8Cd$

anal. calcd., %: C, 57.93; H, 4.32; N, 7.11; Cd, 14.28.

Found, %: C, 57.45; H, 4.56; N, 7.08; Cd, 14.32.

X-ray determination of structure. The single crystal data of the complexes **I** and **II** were collected on a Bruker Smart Apex II CCD diffractometer using the graphite monochromated MoK_{α} radiation ($\lambda = 0.71073 \text{ \AA}$). The data of **I** were collected at 296(2) K. A total of 17626 reections, including 6315 unique reflections ($R_{int} = 0.0163$) were measured in the $1.97^\circ < \theta < 28.34^\circ$. The data of **II** were collected at 296 K. A total of 12540 reections, including 4205 unique reflections ($R_{int} = 0.0290$) were measured in the $1.97^\circ < \theta < 28.34^\circ$. Both structures were solved with a direct method using SHELXS-97 and were refined by full-matrix least-square methods using SHELXTL-97. All H atoms were placed geometrically. The crystallographic data and structure experimental details of the complexes **I** and **II** are given in Table 1, and selected bond lengths and bond angles are presented in Table 2.

Supplementary material for structures **I** and **II** has been deposited with the Cambridge Crystallographic Data Centre (nos. 836989 (**I**) and 836988 (**II**); deposit@ccdc.cam.ac.uk or <http://www.ccdc.cam.ac.uk>).

RESULTS AND DISCUSSION

There are one $[Cd(Bna)(DMF)_2(H_2O)_2]$ and one non-coordinated DMF guest molecules in the asymmetric unit of complex **I**. As shown in Fig. 1, the Cd(II) atom in **I** is coordinated by two oxygen atoms from two carboxylic groups of two independent Bna^{2-} ligands (Cd–O 2.246(2) and 2.260(2) Å), two oxygen atoms from two DMF (Cd–O 2.273(3) and 2.263(2) Å) and two oxygen atoms from two H_2O (Cd–O 2.256(3) and 2.359(2) Å), where the latter two occupy the apical positions to fulfill the octahedron coordination motif. The dihedral angle between the pair of naphthyl rings of the ligand is 88.1° and nearly perpendicular to each other. The selected bond distances and angles of complex **I** are listed in Table 2. The extended structure of **I** features 1D spirals with Cd^{2+} ions as the nodes (Fig. 2a). Here is an 1D channel in the spiral, and the non-coordinated guest DMF molecule is located in the channel by hydrogen bonded to the coordinated water (O...O 2.640 Å). Hydrogen bondings are also found between water molecules from adjacent spiral lines (O...O 2.799 Å) (Fig. 2b). It is interesting that the ligands from the two neighboring spiral are enantiomer, leading to the opposite chirality of these two

Table 1. Crystallographic data and details of the experiment for complexes **I** and **II**

Parameter	Value	
	I	II
Formula weight	740.05	787.09
Crystal system	Monoclinic	Orthorhombic
Space group	$P2_1/n$	$C222_1$
a , Å	12.9178(4)	11.7689(11)
b , Å	11.4056(4)	13.8060(13)
c , Å	23.0528(7)	20.708(2)
β , deg	90.9520(10)	90
Volume, Å ³	3396.02(19)	3364.6(6)
Z	4	4
ρ_{calcd} , g/cm ³	1.447	1.554
μ , mm ⁻¹	0.704	0.711
$F(000)$	1520	1608
Crystal size, mm	0.46 × 0.26 × 0.21	0.27 × 0.09 × 0.08
θ Range for data collection, deg	1.77 to 28.31	1.97 to 28.34
Limiting indices	$-17 < h < 17$, $-15 < k < 14$, $-20 < l < 30$	$-15 < h < 15$, $-8 < k < 18$, $-27 < l < 27$
Reflections collected	21088	12540
Independent reflections	8212 ($R_{\text{int}} = 0.0170$)	4205 ($R_{\text{int}} = 0.0290$)
Completeness to θ , %	97.3	100.0
Goodness-of-fit on F^2	1.053	1.596
Parameters	440	237
Final R indices ($I > 2\sigma(I)$)	$R_1 = 0.0398$ $wR_2 = 0.1085$	$R_1 = 0.0297$ $wR_2 = 0.0568$
R indices (all data)	$R_1 = 0.0498$ $wR_2 = 0.1171$	$R_1 = 0.0349$ $wR_2 = 0.0577$
Largest diff. peak and hole, $e \text{ Å}^{-3}$	1.013 and -0.410	0.939 and -0.333

neighboring spiral lines. These spirals with opposite chirality pack alternatively along y axis (Fig. 2b), makes the structure of complex **I** achiral.

There are $1/2[\text{Cd}(\text{Bna})(\text{Bipy})(\text{DMF})_2]$ in the asymmetric unit of complex **II**. As shown in Fig. 3, the Cd(II) atom in **II** is coordinated by two oxygen atoms from two carboxylic groups of two independent Bna²⁻ ligands (Cd–O 2.3054(19) Å), two oxygen atoms from two DMF (Cd–O 2.330(2) Å) and two nitrogen atoms from two Bipy (Cd–N 2.321(2) and 2.378(2) Å), where the latter two N occupy the apical positions to fulfill the octahedron coordination motif. The dihedral angle between the pair of naphthyl rings of the ligand is 78.6°. The selected bond distances and angles are listed in Table 2. The Cd²⁺ ions connect the adjacent Bna²⁻ ligands to form an infinite 1D zigzag line (Fig. 4a), and then coordinate with Bipy molecules at apical positions to extend to a 2D sheet along y – z

plane (Fig. 4b) with Cd²⁺ ions as the nodes. There isn't strong interactions (H-bonding or p – p stacking) are found between adjacent sheets (Fig. 4c).

Both in **I** and **II**, the phenolic hydroxyl of Bna is uncoordinated with any metal ion, just forms intramolecular hydrogen bondings with O from the adjacent carboxylate groups (O...O 2.52 and 2.56 Å, respectively).

IR study shows that the characteristic absorption band of Bipy gives bands at 1591, 1410, 808, 607 cm⁻¹, while they move to 1581, 1399, 816, 598 cm⁻¹ in complex **II**. This assumed that the N atoms of the Bipy have coordinated with the metal ions.

What's more, IR shows that the characteristic absorption band of C=O gives at 1660 cm⁻¹, C–O gives at 1227 cm⁻¹, while they, respectively, move to 1640 and 1110 cm⁻¹ and from the IR, we observed that the

Table 2. Selected bond lengths (Å) and bond angles (deg) for complexes **I** and **II***

Bond	<i>d</i> , Å	Bond	<i>d</i> , Å
I			
O(11)–Cd(1)	2.272(3)	Cd(1)–O(5)	2.243(2)
Cd(1)–O(10)	2.259(2)	Cd(1)–O(14)	2.360(3)
Cd(1)–O(3)	2.254(3)	Cd(1)–O(1)	2.261(2)
II			
Cd(1)–O(2) ^{#1}	2.3064(19)	Cd(1)–O(2)	2.3064(19)
Cd(1)–O(4) ^{#1}	2.329(2)	Cd(1)–O(4)	2.329(2)
Cd(1)–N(1)	2.325(2)	Cd(1)–N(2) ^{#2}	2.378(2)
Angle	ω, deg	Angle	ω, deg
I			
O(5)Cd(1)O(3)	88.66(12)	O(5)Cd(1)O(10)	89.53(11)
O(5)Cd(1)O(1)	93.30(11)	O(3)Cd(1)O(1)	93.32(14)
O(5)Cd(1)O(11)	178.59(12)	O(3)Cd(1)O(11)	89.94(15)
O(1)Cd(1)O(11)	86.99(12)	O(5)Cd(1)O(14)	93.67(10)
O(10)Cd(1)O(14)	88.01(10)	O(1)Cd(1)O(14)	87.88(11)
O(3)Cd(1)O(10)	90.69(12)	O(10)Cd(1)O(11)	90.27(12)
O(10)Cd(1)O(1)	175.14(11)	O(3)Cd(1)O(14)	177.32(12)
O(11)Cd(1)O(14)	87.72(13)		
II			
O(2) ^{#1} Cd(1)O(2)	166.86(13)	O(2) ^{#1} Cd(1)N(1)	96.57(7)
O(2) ^{#1} Cd(1)O(4) ^{#1}	91.68(8)	O(2)Cd(1)O(4) ^{#1}	87.86(8)
O(2) ^{#1} Cd(1)O(4)	87.85(8)	O(2)Cd(1)O(4)	2.330(2)
O(4) ^{#1} Cd(1)O(4)	175.97(19)	O(2) ^{#1} Cd(1)N(2) ^{#2}	83.43(7)
N(1)Cd(1)N(2) ^{#2}	180.0	O(4) ^{#1} Cd(1)N(2) ^{#2}	87.98(10)
O(2)Cd(1)N(1)	96.57(7)	N(1)Cd(1)O(4)	92.02(10)
C(13) ^{#1} C(14)C(15)	92.02(10)	O(2)Cd(1)N(2) ^{#2}	83.43(7)
O(4)Cd(1)N(2) ^{#2}	87.98(10)		

* Codes symmetry: ^{#1} $-x - 1/2, y - 1/2, -z + 1/2$, ^{#2} $-x - 1/2, y + 1/2, -z + 1/2$ for **I**; ^{#1} $x, -y + 1, -z + 1$, ^{#2} $x + 1, y, z$ for **II**.

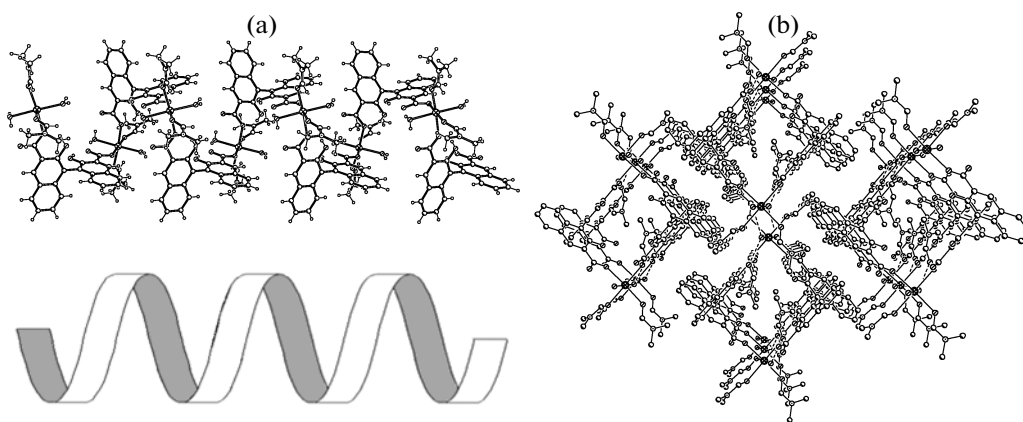


Fig. 2. The 1D spiral structure of **I** (a); the packing arrangement of **I**, viewed along y axis (b).

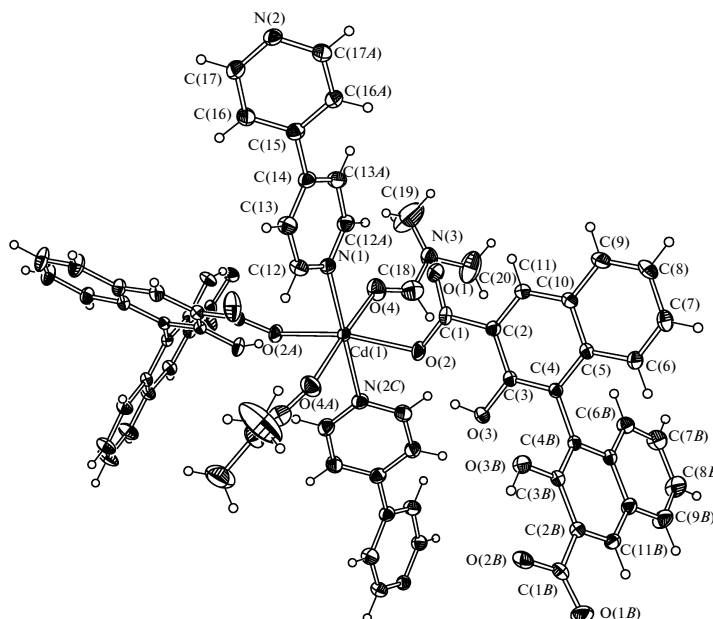


Fig. 3. The coordination environment around Cd(II) in **II** with the thermal ellipsoid at the 30% probability level. Symmetry code: (A) $x, -y + 1, -z + 1$; (B) $-x + 2, y, -z + 3/2$; (C) $x + 1, y, z$.

the characteristic absorption band of phenolic hydroxyl at 1455 cm^{-1} has no change. This assumed that the phenolic hydroxyl was uncoordinated with the metal ions, which assured the freedom of the active centres.

TGA shows that complex **I** is stable up to 110°C . The TG curve of complex **I** showed four weight loss steps (Fig. 5a). The first weight loss of 14.9% from 110 to 150°C is corresponded to the loss of one guest DMF and two water molecules. The second weight loss of 23.4% between 153 and 275°C is attributed to the loss of two DMF molecules. The last weight loss of 46.7% is attributed to the loss of all organic ligands and the residue is CdO.

TGA shows that complex **II** (Fig. 5b) is stable up to 200°C . The TG curve of complex **II** showed three weight loss steps. The first weight loss of 23.02% from 205 to 265°C is corresponded to the loss of two DMF molecules. The second weight loss of 5.51% between 265 and 324°C is attributed to the loss of one Bipy molecule. The third weight loss of 57.56% is attributed to the loss of all organic ligands and the residue is CdO.

We comprised the imitation and actual measurement XRPD pattern of complex **II**. The results assume that the individual single crystalline structural

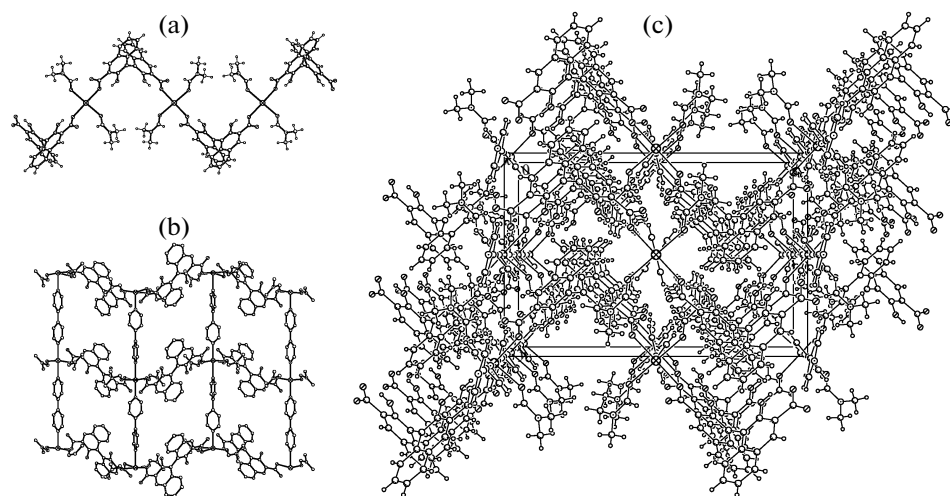


Fig. 4. The 1D $-\text{Cd}-\text{Bna}-\text{Cd}-$ zigzag line of **II** (a); schematic representation of the 2D chiral sheet (b); the packing arrangement of **II**, viewed along the x axis (c).

is as the same as the huge mass small crystalline structural.

ACKNOWLEDGMENTS

This work was supported by the Natural Science Foundation of Hebei Province (nos. B2010000223, B2012201109).

REFERENCES

1. Yaghi, O.M., O'Keeffe, M., Ockwig, N.W., et al., *Nature*, 2003, vol. 423, p. 705.
2. Férey, G., Mellot-Draznieks, C., Serre, C., et al., *Science*, 2005, vol. 309, p. 2040.
3. Kitagawa, S., Kitaura, R., and Noro, S., *Angew. Chem. Int. Ed.*, 2004, vol. 43, p. 2334.
4. Moulton, B. and Zaworotko, M.J., *Chem. Rev.*, 2001, vol. 101, p. 1629.
5. Yaghi, O.M., O'Keeffe, M., Eddaoudi, J., et al., *Nature*, 2003, vol. 423, p. 705.
6. Hill, R.J., Long, D.L., Champness, N., et al., *Acc. Chem. Res.*, 2005, vol. 38, p. 335.
7. Bradshaw, D., Warren, J.E., and Rosseinsky, M.J., *Science*, 2007, vol. 315, p. 977.
8. Evans, O.R. and Lin, W., *Acc. Chem. Res.*, 2002, vol. 35, p. 511.
9. Férey, G., Mellot-Draznieks, C., Serre, C., and Millange, F., *Acc. Chem. Res.*, 2005, vol. 38, p. 217.
10. Rosi, N.L., Eckert, J., Eddaoudi, M., et al., *Science*, 2003, vol. 300, p. 1127.
11. Kesanli, B., Cui, Y., Smith, M.R., et al., *Angew. Chem. Int. Ed.*, 2005, vol. 44, p. 72.
12. Chen, B., Zhao, X., Putkham, A., et al., *J. Am. Chem. Soc.*, 2008, vol. 130, p. 6411.
13. Pan, L., Parker, B., Huang, X., et al., *J. Am. Chem. Soc.*, 2006, vol. 128, p. 4180.
14. Dybtsev, D.N., Nuzhdin, A.L., Chun, H., et al., *Angew. Chem. Int. Ed.*, 2006, vol. 45, p. 916.
15. Cho, S.H., Ma, B.Q., Nguyen, S.T., et al., *Chem. Commun.*, 2006, p. 2563.
16. Wu, C. and Lin, W., *Angew. Chem. Int. Ed.*, 2007, vol. 46, p. 1075.
17. Wu, C., Hu, A., Zhang, L., and Lin, W., *J. Am. Chem. Soc.*, 2005, vol. 127, p. 8940.

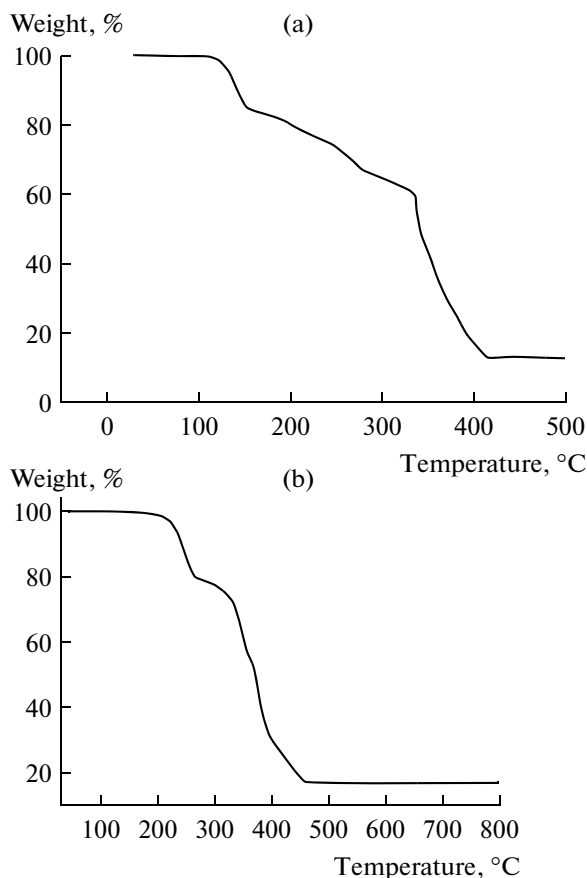


Fig. 5. The thermogravimetric curves of complexes **I** (a) and **II** (b).